Journal of Applied Electrochemistry **31**: 65–72, 2001.

Influence of heat treatment on the corrosion of high speed steel

V.A. ALVES[1], C.M.A. BRETT[1]* and A. CAVALEIRO[2]
[1]*Departamento de Química, Universidade de Coimbra, 3004-535 Coimbra, Portugal*
[2]*Departamento de Engenharia Mecânica, Universidade de Coimbra, 3030 Coimbra, Portugal*
*(*author for correspondence, fax: +351 239 835295, e-mail: brett@ci.uc.pt)*

Received 18 April 2000; accepted in revised form 19 July 2000

Key words: corrosion, electrochemical methods, heat treatment, high speed steel, pitting

Abstract

The corrosion behaviour of M2 high speed steel, as-received as well as heat-treated under different conditions, has been studied in 0.1 M KCl aqueous solution by corrosion potential measurements, Tafel curves and electrochemical impedance. Heat treatment leads to an increase of the corrosion resistance of high speed steel; the higher the tempering temperature after quenching, the higher the corrosion resistance of the steel. X-ray diffraction, energy dispersive X-ray analysis and scanning electron microscopy were also used to further understand the corrosion behaviour of the different samples. Based on these analyses, the microstructure of the different samples was correlated with their corrosion properties.

1. Introduction

A general problem with engineering alloys of great utility in industry, such as stainless steels and Al alloys, is that in certain environments they are attacked, particularly by pitting corrosion. A recent review focusing on these types of alloy summarises the effects of a number of critical factors in pitting corrosion [1]. Considerable effort has been devoted to understanding the pitting phenomenon in recent decades, but an in-depth description of some of the many steps involved is still lacking. The most studied metals have been aluminium and its alloys and stainless steels, because of their practical importance.

Examples of pitting corrosion studies on stainless steels include [2–8]. However, little attention has been paid to other types of steel. There are, however, a few electrochemical corrosion studies of carbon steel [9–11] as well as of high speed steel [12]. Such studies are of fundamental importance, since these types of steel are used as substrates for the deposition of thin-film coatings, which are applied in order to improve their mechanical properties (wear, hardness) as well as their corrosion resistance. In the last few years some investigations have been reported on coated carbon steel [13–16] and on coated high speed steel [16–22].

From the literature [23], it is known that high speed steel (HSS) has a multiphase structure, which is highly influenced by the thermal treatment employed. In the present work, the influence of heat treatment on the corrosion properties of HSS has been studied. As-received HSS and HSS tempered at different temperatures after quenching have been investigated, in order to examine how the heat treatment influences the corrosion properties and, in turn, if these features are reflected in the steel microstructure.

2. Experimental details

M2 high speed steel (W 6.4; Mo 5.0; Cr 4.2; V 1.9; C 0.86 wt %) as-received, as well as submitted to different heat treatments was used in this work. The heat treatment consisted of the following steps: (a) austenitizing at 1150 °C for 10 min in argon atmosphere, (b) quenching in oil down to room temperature and (c) triple tempering (2 h + 2 h + 2 h). Two tempering temperatures were studied, 550 and 650 °C. The samples, discs of area 1.8 cm^2 and 1.0 mm thickness, were polished with silicon carbide papers of various grit sizes (240, 320, 600, 800, 1200 and 2500), and finally with diamond paste of 6 μm diameter particle size, until a mirror finish was obtained. They were then rinsed with acetone and ultrapure water. Electrodes were prepared from discs by attaching a copper wire to the rear with silver epoxy and covering with epoxy resin; the edges were coated with varnish, leaving just one face exposed. A 0.1 M KCl aqueous solution was used as the aggressive medium, which was prepared using analytical grade reagent and Millipore Milli-Q water (resistivity > 18 MΩ cm). Solutions were not deaerated.

A three-electrode cell containing a Pt foil auxiliary electrode and a saturated calomel reference electrode was employed. Corrosion potential and polarization

curve experiments were done using a EG&G PAR 273A potentiostat with M352 corrosion analysis software. Impedance experiments were carried out with a Solartron 1250 frequency response analyser coupled to a Solartron 1286 electrochemical interface, with a 5 mV r.m.s. perturbation, from 65 kHz down to 100 mHz. Experiments were controlled with ZPlot software and fitting was performed with ZSim CNLS software.

Scanning electron microscopy was carried out on a Jeol T330 scanning electron microscope equipped with a Tracor Northern microanalysis accessory. X-ray diffraction analysis was done using a Philips PW3040/00 X-Perth diffractometer.

3. Results and discussion

3.1. *Open circuit potential*

The corrosion potential, E_{cor}, at open circuit potential as a function of time for high speed steel submitted to different heat treatments is shown in Figure 1. A significant variation of potential to more negative values is observed during the first hour of immersion, reaching almost stable values after 4 h immersion. The behaviour of samples after 650 °C heat treatment is in agreement with that previously observed for HSS in chloride solution [12].

The E_{cor} values for HSS show a tendency to more positive values in the order: as-received < heat-treated at 550 °C < heat-treated at 650 °C (Table 1).

3.2. *Potentiodynamic behaviour*

Polarization curves were recorded for the different samples of HSS to obtain the Tafel parameters. Figure 2 shows the curves obtained for three different immersion times: 10 min, 1 h and 4 h. It can be seen that after 1 h immersion the curves are almost superimposed.

The fitting of the curves close to the corrosion potential was done using M352 ParCalc software to obtain values of corrosion currents and corrosion

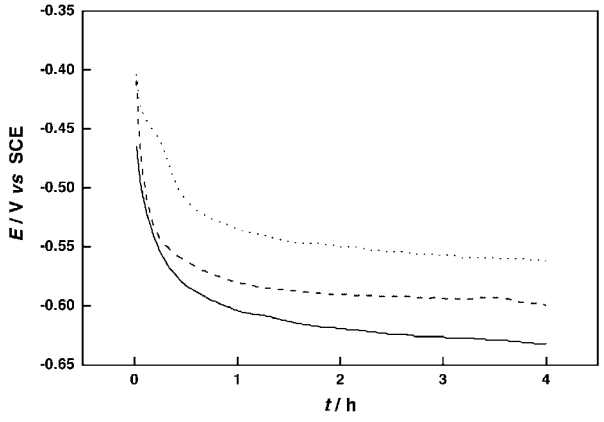

Fig. 1. Variation of open circuit corrosion potential, E_{cor}, against time of high speed steel in 0.1 M KCl solution. (——) as-received; (- - - -) heat-treated at 550 °C; (····) heat-treated at 650 °C.

Table 1. Values of E_{cor} (vs SCE) from open circuit potential measurements

Type of sample	$-E_{cor}$/V vs SCE	
	10 min	4 h
1	0.54	0.63
2	0.53	0.60
3	0.45	0.56

1: as-received HSS; 2: HSS heat-treated at 550 °C; 3: HSS heat-treated at 650 °C

potentials, see Table 2. After 10 min immersion, a positive shift in E_{cor} with heat-treated samples similar to that found in the case of E_{cor} from open circuit vs time measurements was observed. It can be seen that heat-treated HSSs have lower I_{cor} values than in the as-received state, suggesting that heat treatment decreases the steel corrosion rate. After 10 min and 4 h immersion the I_{cor} values are lowest for HSS tempered at 650 °C. There is a tendency of increasing I_{cor} with immersion time, which is in agreement with the fact that the E_{cor} values become more negative as a function of time.

Polarization resistance values, R_p, were obtained from I against E curves and are in good agreement with the other results obtained. The highest R_p values after 1 h and 4 h immersion for HSS heat-treated at 650 °C, in comparison with the values obtained for the other samples, corroborate their lowest I_{cor} values, especially when compared with that of as-received HSS (Table 2).

3.3. *Electrochemical impedance spectroscopy*

Impedance spectra were obtained at the open circuit potential for the HSS samples after 10 min, 1 h and 4 h immersion. The general shape of the spectra is the same for all samples; Figure 3 shows the representative impedance behaviour of HSS.

Fitting of the spectra was done by using a simple equivalent circuit, composed of an *RC* parallel combination in series with the solution resistance. This same type of model has been previously used for HSS [12]. The calculated R and C values are shown in Table 3. The capacitance was represented by a constant phase element (*CPE*) in order to take into account its frequency dispersion behaviour, which is normally found for solid electrodes. The extent of this dispersion is often related directly to the roughness of the electrodes [24]; however, evidence has been found that the origin of the capacitance dispersion may depend more on atomic-scale inhomogeneities [25]. The *CPE* exponent found here had values between 0.84 and 0.71 with a tendency to decrease with immersion time.

The charge transfer resistance values, R_{ct}, are in general higher for heat-treated HSS (550 °C and 650 °C) when compared with as-received HSS, which is in agreement with the lowest I_{cor} values found for these heat-treated samples from the Tafel curves. The capacitance of the steel-solution interface increases with

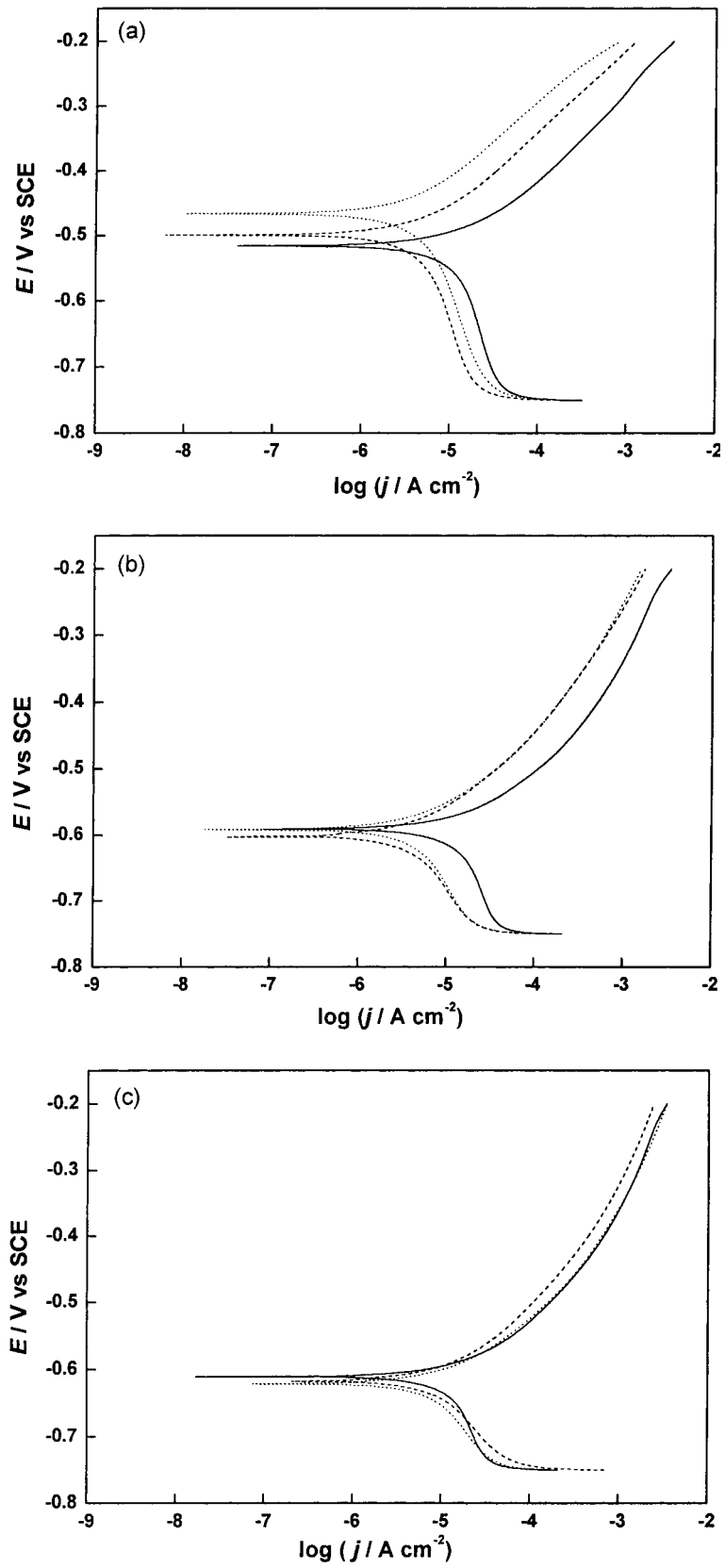

Fig. 2. Tafel plots for HSS samples after immersion in 0.1 M KCl solution for (a) 10 min, (b) 1 h, (c) 4 h (——) as-received; (- - - -) heat-treated at 550 °C; (····) heat-treated at 650°C. Scan rate 2.5 mV s^{-1}.

immersion time, which suggests an increase of the steel surface area. It is thought that the growing of pits on the steel surface as well as the accumulation of corrosion products around them, which in turn presents a porous nature, can lead to an increase of the steel surface area, although it was not measured in the present work.

Table 2. Corrosion parameters obtained from analysis of the Tafel curves

Type of sample	$I_{cor}/\mu A\ cm^{-2}$			$-E_{cor}/V$ vs SCE		
	10 min	1 h	4 h	10 min	1 h	4 h
1	19.0	30.6	32.4	0.52	0.59	0.61
2	13.5	11.2	17.7	0.50	0.60	0.62
3	11.2	15.4	16.2	0.47	0.59	0.62

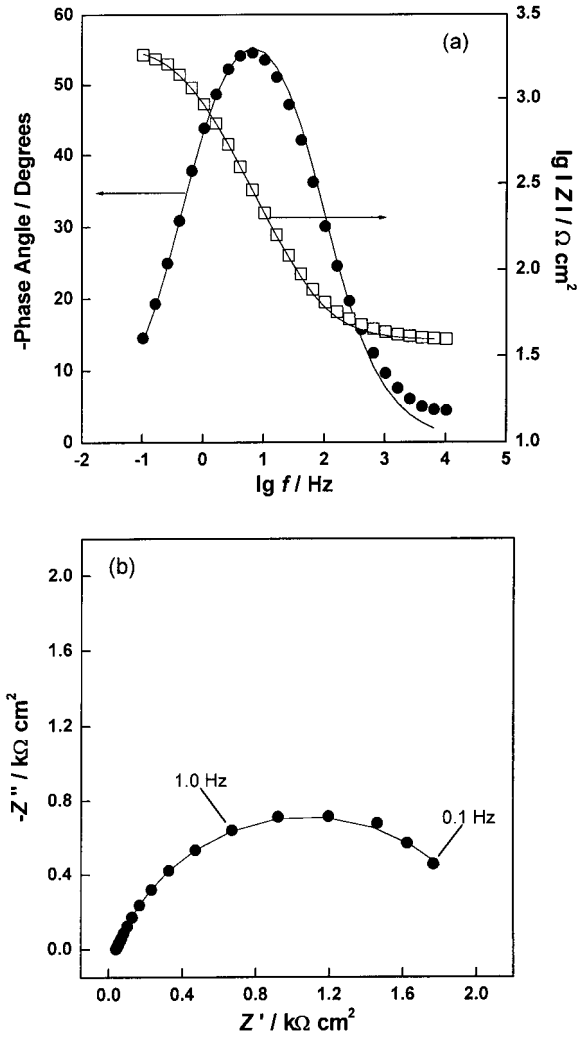

Fig. 3. Impedance spectra at open-circuit potential for HSS heat-treated at 650 °C after 10 min immersion in 0.1 M KCl solution. (a) Bode and (b) complex plane plots. Solid lines show the fitting to the equivalent circuit.

Table 3. Values of charge transfer resistance, R_{ct}, of the corrosion process and capacitance of the steel-solution interface, C, obtained from the analysis of the impedance spectra

Type of sample	$R_{ct}/k\Omega\ cm^2$			$C/mF\ cm^{-2}$		
	10 min	1 h	4 h	10 min	1 h	4 h
1	1.81	1.33	1.73	0.72	0.80	1.32
2	1.66	1.77	1.84	0.44	0.88	1.31
3	2.08	1.64	1.69	0.20	0.62	0.84

The lowest C values for HSS tempered at 650 °C indicate that its surface has suffered a less aggressive corrosion attack, as observed by visual inspection.

3.4. *X-ray diffraction (XRD) analysis before and after pitting corrosion*

Microstructural analysis of HSS by XRD evidenced the presence of two types of carbide phase: M_6C (M = W, Cr, Mo or Fe, principally Fe_3W_3C [26]) and V_4C_3 [27], as well as Fe diffraction lines, as shown in Figure 4(a) for an as-received HSS sample. This HSS multiphase structure has been previously reported [23]. The same microstructure was observed for all HSS samples (Figure 4(b)). However, the peaks due to the ferritic (tempered martensite) matrix are more intense and narrower for as-received HSS.

The lower crystallinity of the samples which were submitted to heat treatment can be related to the large number of defects formed after quenching, characteristic of the martensitic phase. In spite of the recovery of the structure during tempering, some distortion is always present in the tempered martensitic matrix. The main contribution to the lattice distortion of the martensitic matrix is the presence of carbon in interstitial positions. Tempering at 650 °C seems to be more efficient than at 550 °C and leads to narrower diffraction peaks. This can be related to the different ferrite crystallite sizes at 550 °C and 650 °C, which were obtained from the Sherrer formula [28]:

$$t = \frac{0.9\,\lambda}{B\cos\theta_B} \tag{1}$$

where t is the crystallite size in nanometre (nm), λ is the radiation wavelength (0.178 896 nm), B is the peak width, in radians, where the intensity corresponds to half that of the maximum intensity, and θ_B is the angle where the intensity is maximum. The higher value of crystallite size found for HSS tempered at 650 °C (t = 45 nm), when compared to that of HSS tempered at 550 °C (t = 28 nm), can explain the narrower and more intense peaks found for this sample.

The HSS samples were also analysed after corrosion to identify the crystalline nature of the corrosion products (or oxides), which could be seen by visual observation. Figure 4(c) shows diffractograms, before and after corrosion, for an HSS sample heat-treated at 550 °C. The low intensity peak appearing after corrosion was identified as iron oxide hydrate, FeO(OH) [29]. This corrosion product has also been observed after corrosion of hard thin sputtered films of W–Ti and W–Ti–N on HSS [20].

3.5. *Morphological (SEM) and chemical (EDS) observations after pitting corrosion*

All HSS samples suffered from pitting corrosion during the various electrochemical experiments. At the end of the experiments the pit diameter was of the order of

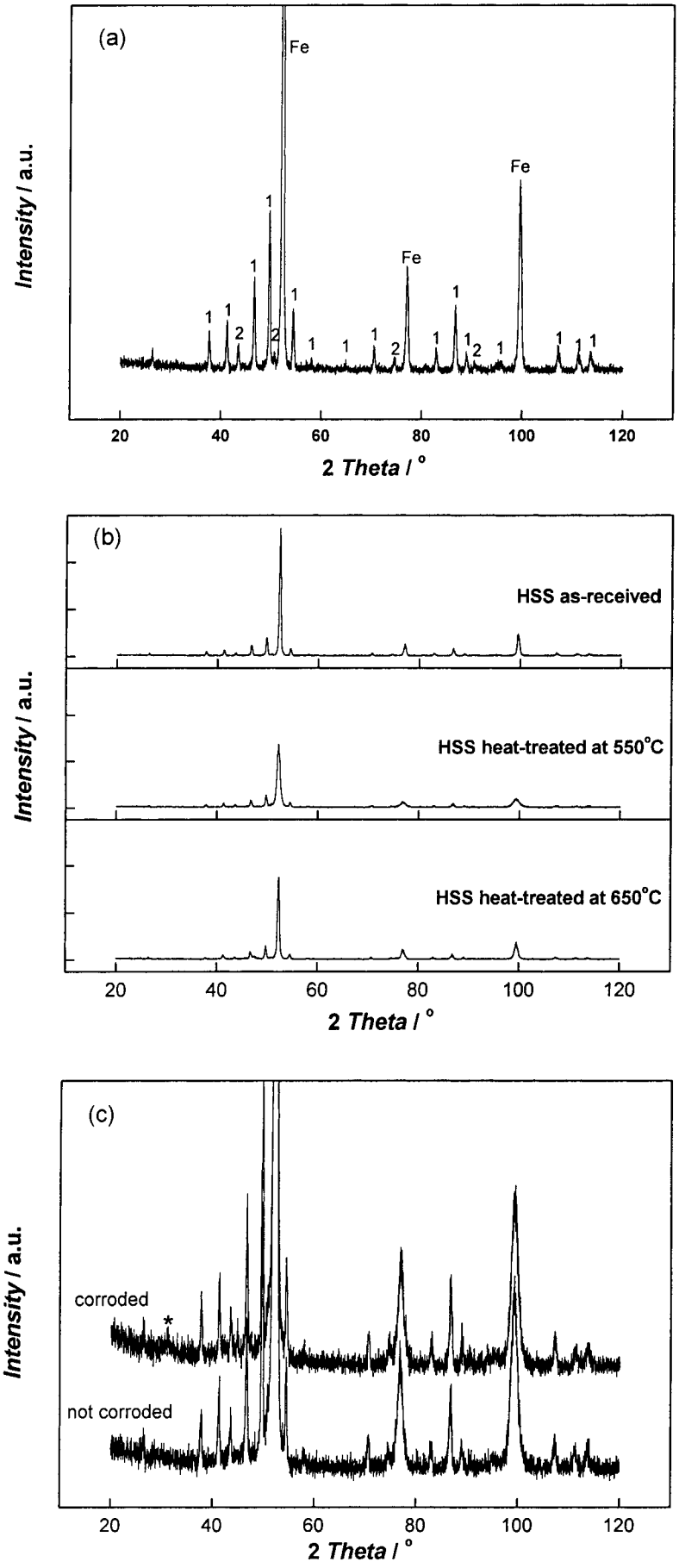

Fig. 4. X-ray diffraction patterns of: (a) as-received HSS. 1: M_6C; 2: V_4C_3; (b) different types of uncorroded HSS sample; (c) HSS heat-treated at 550 °C; ∗: peak due to iron oxide hydrate, which appeared after corrosion.

several micrometers; measuring the exact diameter of the pits is difficult due to the accumulation of corrosion products around and/or over the pit. Figure 5 shows details of the localised corrosion of HSS samples. Figure 5(a) shows a typical pit at the centre of a circular ring consisting of corrosion products. In the interior of a pit a 'mud-cracked' structure can be seen, over which the carbides are now clearly in evidence (Figure 5(b)).

The EDS spectrum (Figure 6(a)) obtained inside a corroded zone surrounded by corrosion products (as in Figure 5(a)) shows a significant contribution from the alloying elements present in high speed steel, confirming earlier results [12]. The ferritic matrix is preferentially attacked rather than the carbide phases present in the steel microstructure (see XRD analysis), which remain practically untouched, as shown in Figure 5(b). Thus, the *EDS* spectrum obtained outside the corroded zone, Figure 6(b), shows evidence of a higher contribution from iron, in comparison with that of the alloying elements.

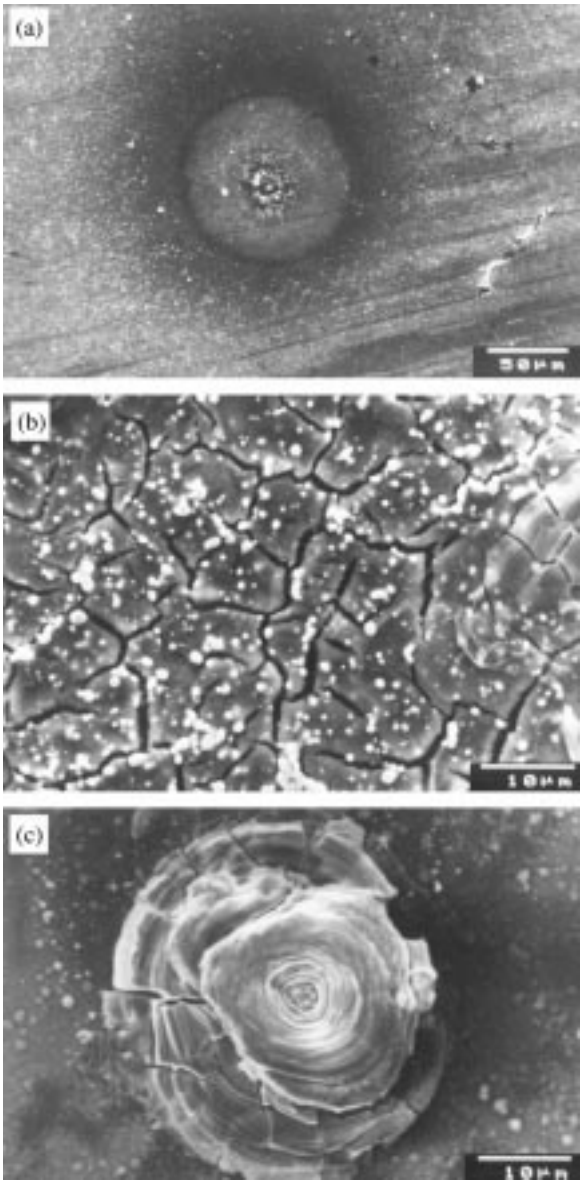

Fig. 5. Representative SEM micrographs on the corrosion of HSS. (a) Pit at the centre of a circular ring consisting of corrosion products (HSS heat-treated at 650 °C); (b) interior of a pit (HSS heat-treated at 550 °C); (c) the 'rose' structure (region near a corroded zone, HSS heat-treated at 550 °C).

The presence of structures with a shape similar to a 'rose' was also observed, see Figure 5(c) for an example. These structures are formed near to the steel corroded zones and consist almost exclusively of corrosion products (see EDS spectrum, Figure 6(c)). This suggests that pitting corrosion induces propagation of the corrosive attack in the neighbourhood of the pit, with formation of corrosion products having a well-defined morphology and exhibiting essentially two-dimensional growth. This is probably linked to the adsorption of chloride ions by the freshly precipitated hydroxides [30].

3.6. *Comparative remarks*

The various electrochemical techniques employed all show that heat treatment of high speed steel leads to a higher corrosion resistance of the samples, particularly regarding pitting corrosion. The reason for such an improvement has to be traced to alterations in the microstructure of the steel, and is probably related to the fact that a higher quantity of alloying elements remains in solid solution in the ferritic matrix, in comparison with the as-received condition.

The structural evolution during tempering for this particular steel is very complex [23, 31, 32]. In the as-received condition, the ferritic matrix does not contain any carbon, all the carbon being present in the form of carbides. During austenitising at 1200 °C, most of the primary carbides (M_6C, $M_{23}C_6$ and M_4C_3, M = Cr, W, Mo, V) is dissolved. In particular, $M_{23}C_6$, a mixed carbide very rich in chromium, is totally dissolved. At this temperature, the C content in the austenite matrix reaches 0.8 wt %, whereas Cr, Mo, W and V attain 4.2, 3.2, 3.6 and 1.2 wt %, respectively [32]. Consequently, after quenching from the austenitising temperature, both the retained-austenite matrix and the martensite are very rich in alloying elements. During tempering (triple treatment), decomposition of the martensite and transformation of the austenite are observed. The evolution of the structure with tempering temperature can be summarized as follows:

(i) 80 °C < t < 200 °C, formation of the ε ($Fe_{2.4}C$) carbide.
(ii) 235 °C < t < 355 °C, formation of the M_3C carbide (very rich in Fe).
(iii) 400 °C < t < 500 °C, progressive enrichment of M_3C carbide in Cr and transformation into $M_{23}C_6$.
(iv) 525 °C < t < 575 °C, precipitation of the secondary carbide M_4C_3 (very rich in V and Cr). This carbide is responsible for the secondary hardening observed in this type of steel.
(v) 575 °C < t < 700 °C, redissolution of M_4C_3 and part of $M_{23}C_6$ carbides.
(vi) t > 700 °C, formation of M_6C (rich in Mo and W) and $M_{23}C_6$, coalescence of carbides.

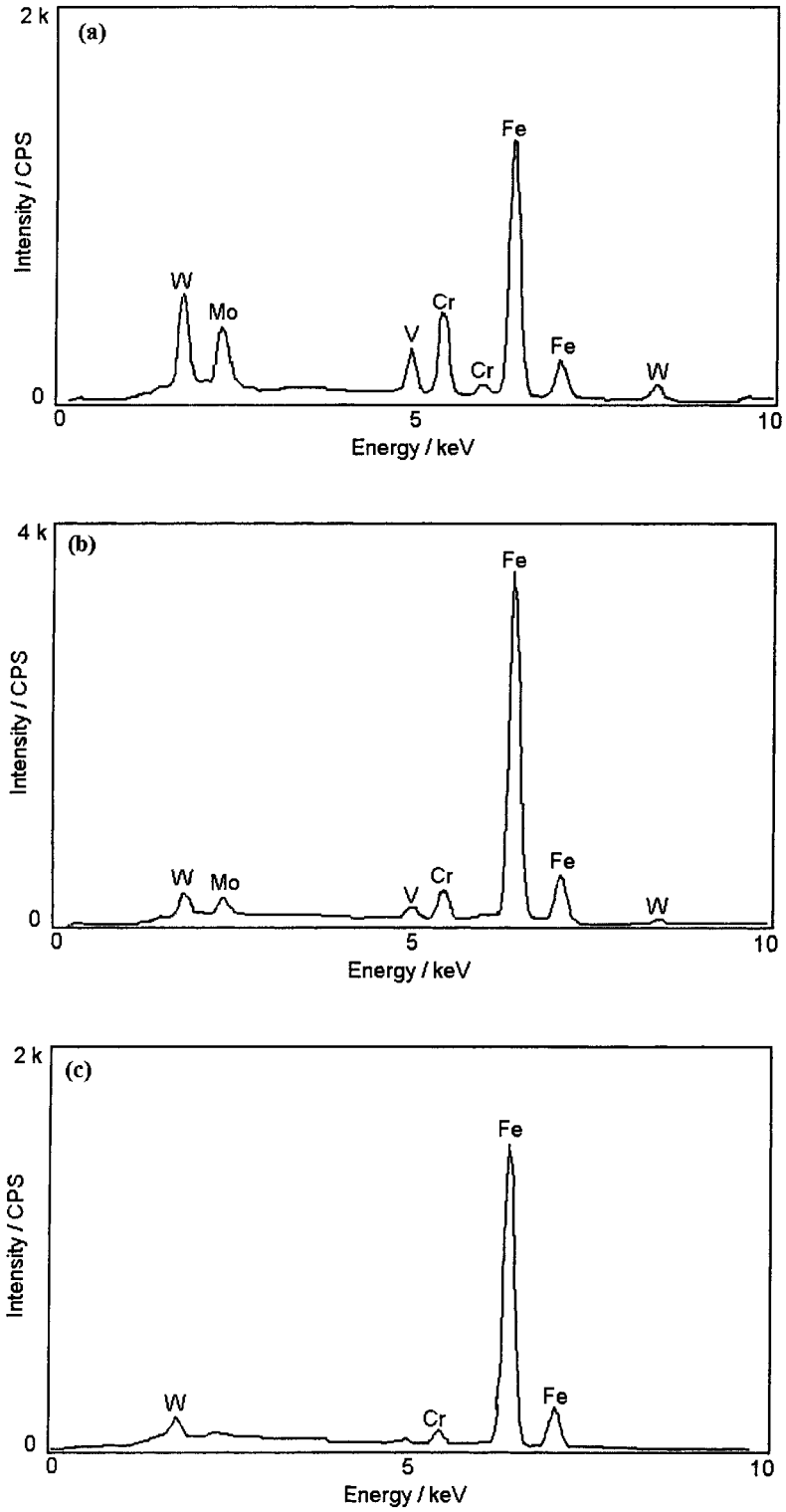

Fig. 6. EDS spectra obtained at specific points of the corroded HSS samples. (a) Inside a pit; (b) outside of a corroded zone; (c) spectrum of a 'rose'. (HSS heat-treated at 550 °C).

Thus, the corrosion behaviour can be understood as follows. (a) After thermal treatment (for both 550 °C and 650 °C), there is a higher alloying element content in the tempered martensite matrix than in the as-received condition (note that for temperatures higher than 650 °C carbide precipitation from the tempered martensite continues, signifying that the amount of alloying elements in the matrix is still very high). Since the beneficial influence of these elements, particularly chromium, on the corrosion resistance of steels can be expected only if they are in solid solution in the iron matrix, the corrosion behaviour should be better. (b) Redissolution of M_4C_3 and part of the $M_{23}C_6$ carbides in the temperature range 575 °C $< t <$ 700 °C leads to

an increase of the fraction of alloying elements in the tempered martensite matrix. Thus, a higher corrosion resistance should be expected after tempering at 650 °C than after tempering at 550 °C.

The conclusion that corrosion resistance can be improved by procuring heat treatment conditions in which the alloying elements remain in solid solution may be generally applicable.

4. Conclusions

Electrochemical measurements have shown that heat treatment of high speed steel leads to a lower susceptibility to pitting corrosion in chloride media, and which depends on the heat treatment temperature. From surface analysis and microscopic techniques, it has been shown that these results can be correlated with the changed steel microstructure. The main reason for such an improvement is traced to the higher fraction of alloying elements remaining in solid solution in the ferritic matrix.

Acknowledgements

The authors thank Instituto de Ciência e Engenharia de Materiais e Superfícies, University of Coimbra for financial support. V.A.A. thanks CNPq (Brazil), project 200396/99-4, for a post-doctoral fellowship. The authors thank Prof. M.T. Vieira for helpful discussions regarding the structure and morphology of heat-treated steels.

References

1. G.S. Frankel, *J. Electrochem. Soc.* **145** (1998) 2186.
2. T. Hong and M. Nagumo, *Corros. Sci.* **39** (1997) 285.
3. T. Hong and M. Nagumo, *Corros. Sci.* **39** (1997) 1665.
4. I. Annergren, D. Thierry and F. Zou, *J. Electrochem. Soc.* **144** (1997) 1208.
5. R.P. Vera Cruz, A. Nishikata and T. Tsuru, *Corros. Sci.* **40** (1998) 125.
6. R. Qvarfort, *Corros. Sci.* **40** (1998) 215.
7. M.K. Ahn, H.S. Kwon and H.M. Lee, *Corros. Sci.* **40** (1998) 307.
8. M. da Cunha Belo, B. Rondot, C. Compere, M.F. Montemor, A.M.P. Simoes and M.G.S. Ferreira, *Corros. Sci.* **40** (1998) 481.
9. A. Bonnel, F. Dabosi, C. Deslouis, M. Duprat, M. Keddam and B. Tribollet, *J. Electrochem. Soc.* **130** (1983) 753.
10. M. Ergun and A.Y. Turan, *Corros. Sci.* **32** (1991) 1137.
11. Y.F. Cheng and J.L. Luo, *J. Electrochem. Soc.* **146** (1999) 970.
12. C.M.A. Brett and P.I.C. Melo, *J. Appl. Electrochem.* **27** (1997) 959.
13. M. Uergen and A.F. Cakir, *Surf. Coat. Technol.* **96** (1997) 236.
14. L.A.S. Ries, D.S. Azambuja and I.J.R. Baumvol, *Surf. Coat. Technol.* **89** (1997) 114.
15. E. Lunarska and J. Michalski, *J. Mater. Sci.* **30** (1995) 4125.
16. L.F. Senna, C.A. Achete, T. Hirsch and F.L. Freire Jr., *Surf. Coat. Technol.* **94–95** (1997) 390.
17. S.C. Lee, W.Y. Ho and F.D. Lai, *Mater. Chem. Phys.* **43** (1996) 266.
18. C.M.A. Brett and A. Cavaleiro, *Mater. Sci. Forum* **192-4** (1995) 797.
19. C.M.A. Brett and C.-M. Nimigean, *Thin Solid Films* **311** (1997) 1.
20. C.M.A. Brett and A. Cavaleiro, *Thin Solid Films* **322** (1998) 263.
21. A. Cavaleiro, C. Louro, V. Fernandes and C.M.A. Brett, *Vacuum* **52** (1999) 157.
22. J.C. Oliveira, A. Cavaleiro and C.M.A. Brett, *Corros. Sci.*, **42** (2000) 1881.
23. G. Barreau, M.L. Joyeux, T. Vieira and G. Cizeron, *Traitement Thermique* **149** (1980) 45.
24. R. de Levie, *Electrochim. Acta* **9** (1964) 1231.
25. Z. Kerner and T. Pajkossy, *J. Electroanal. Chem.* **448** (1998) 139.
26. Joint Committee on Powder Diffraction Standards, Powder Diffraction File, International Centre for Diffraction Data, Swarthmore, PA, USA, Card 41-1351.
27. Joint Committee on Powder Diffraction Standards, Powder Diffraction File, International Centre for Diffraction Data, Swarthmore, PA, USA, Card 1-1159.
28. B.D. Cullity, 'Elements of X-Ray Diffraction' (Addison-Wesley, CA, 1978), p. 102.
29. Joint Committee on Powder Diffraction Standards, Powder Diffraction File, International Centre for Diffraction Data, Swarthmore, PA, USA, Card 8-98.
30. G. Pajonk and H.-D. Steffens, *Fresenius' J. Anal. Chem.* **358** (1997) 285.
31. M.T. Vieira, PhD thesis, Université Paris Sud, Centre d'Orsay, Paris, France (1983).
32. M.T. Vieira, F. Charpentier and G. Cizeron, *Memoires et Études Scientifiques, Revue de Metalurgie* **10** (1983) 567.